Journal of Harbin Engineering University
ISSN: 1006-7043

Vol 47 No.01
January 2026

Throughput Optimization for Non-Linear Energy Harvesting Based Cooperative Device-to-Device Network using Time Switching Scheme

[1]Gbenga Ayodeji Gbotoso, [2*] Damilare Oluwole Akande, [2] Zachaeus Kayode Adeyemo

[1] Department of Electrical and Electronic Engineering, Lagos State University of Science and Technology, Ikorodu, Lagos State, Nigeria.

[2]Department of Electronic and Electrical Engineering, Ladoke Akintola University of Technology. Ogbomoso, Oyo State, Nigeria

*Corresponding author

Abstract

Providing an achievable throughput performance with optimal resource allocation in energy constrained device-to-device (D2D) wireless communication via Energy harvesting (EH) scheme with sustainable lifetime extension is of curial concern. However, existing resource allocation methods used to achieve throughput performance is limited due to the impractical characteristic behaviour experienced in conventional EH models and the intractable complex characteristic of the non-linear model. These limitations have hindered the performance of simultaneous wireless information and power transfer (SWIPT) enabled D2D networks in attaining its optimal throughput performances. In this paper, the performance of Time Switching (TS) scheme on D2D relaying network using the piecewise linear EH model for Amplify-and-Forward (AF) protocol was performed. An achievable throughput maximization problem was formulated based on available instantaneous channel state information (CSI) and the solution was derived in terms of optimal TS ratio and allocated power. A resource allocation algorithm was proposed for the management of the derived solution. Simulation results obtained revealed that the developed resource allocation algorithm achieved a better throughput performance than the existing linear and non-linear EH models.

Keywords: Device-to-Device, Energy Harvesting, Resource Allocation, Throughput

1. Introduction

As wireless communication systems develop rapidly, the projected growth to over 8 trillion mobile users by 2030 [1] will place significant strain on Internet of Things (IoT) networks to satisfy increasingly demanding throughput needs. IoT applications are expanding in scale across diverse sectors such as residential, industrial, and financial domains. Although numerous wireless technologies which include Bluetooth, ZigBee, and Wi-Fi have been developed for IoT, many rely on unlicensed frequency bands, which often cannot guarantee consistent quality of service (QoS) [2, 3]. To address this, Device-to-Device (D2D) communication which is one of the key components of 5G technology is expected to support many IoT systems by offloading traffic from cellular networks [4]. By enabling nearby devices to communicate directly, D2D improves cellular throughput, reuses licensed spectrum efficiently, and reduces reliance on base station routing [1].

Mobile devices are energy-constrained, creating a critical need for reliable power at communication terminals. While studies have considered conventional sources like solar and wind energy, these are hindered by the mobility of D2D nodes [5]. Consequently, Simultaneous Wireless Information and Power Transfer (SWIPT) has become a key research focus. SWIPT can extend network lifetime [6] and is uniquely available for mobile D2D devices, even when traditional energy sources are not [7, 8]. Importantly, various research shows that SWIPT can satisfy Quality of Service (QoS) and security requirements in critical, energy-constrained scenarios, including in cognitive radio networks [9], wireless cooperative networks [10,11], and non-orthogonal multiple access (NOMA) systems [12]. The two fundamental schemes for SWIPT are Time Switching (TS) and Power Splitting (PS) [13, 14]. TS operates in the time domain, switching between energy harvesting and information reception. In contrast, PS operates in the power domain, dividing the incoming signal for concurrent energy and information processing.

In addition, SWIPT can also categorized according to linear or nonlinear model based on the rectifier's characteristics [15]. The linear model, extensively explored in earlier literature, assumes a direct, proportional relationship between input radio frequency (RF) power and harvested direct current (DC) power. However, this simplification fails to capture the

impracticalities of actual EH circuitry. As a result, recent research interest prioritizes the nonlinear model, which incorporates the essential nonlinear dynamics of rectifying components such as diodes and capacitors. The design of SWIPT schemes for cooperative relaying networks has been extensively explored and are reviewed therein. In the work of [11], the closed form expressions for the optimal TS and PS ratios were derived to optimize the ergodic throughput and outage probability in AF relaying networks using the linear EH model.

Salim *et al*. [16] studied EH in cooperative D2D networks using a linear EH model with PS. The paper examined how the distance between the D2D transmitter and receiver affects both the network data rate and the energy harvested at the relay node. However, the linear model overestimated the harvested energy and misrepresent the data rate relative to network parameters leading to inefficient resource allocation. Boshkovska *et al*. [17] analyzed resource allocation using a logistic nonlinear EH model, formulating an algorithm to maximize harvested power under Signal to Interference Noise Ratio (SINR) constraints. The results showed the logistic model surpasses a linear EH model in performance. However, the logistic nonlinear model's harvested energy curve remains an approximation, failing to fully capture actual circuit behavior due to the complexity of the optimization problem.

Bai *et al*. [18] examined the performance of logistic nonlinear and fractional EH models for AF relaying with a direct link. The paper analyzed resource allocation for both models using the PS scheme based on system capacity. Although both nonlinear models outperformed the linear EH model, they introduced significant computational complexity in achieving the optimal system capacity. The author in [19] studied linear and logistic nonlinear EH models in concurrent cellular and D2D communications over Rayleigh fading channels. The work analyzed the total throughput and harvested energy under both TS and PS schemes for each model. The authors derived closed-form expressions for achievable throughput under both EH models for cellular and D2D links. Results indicated that the logistic nonlinear model provides a much closer approximation to practical EH circuit behaviour and achieves higher throughput compared to the linear model. However, the logistic nonlinear model's analytical complexity makes it less tractable for optimization. Lu *et al*. [20] optimized throughput in a HD, AF relaying network using PS and TS EH schemes under a piecewise linear EH model at the relay. The throughput under each scheme was analyzed and compared with traditional linear EH for resource allocation. Results indicated that the piecewise linear model outperforms the linear model, with PS surpassing TS under low noise conditions and TS performing better under relatively high noise. However, the study did not consider the effect of interference on network performance.

Babaei *et al*. [21] analyzed the performance of dual-hop AF relaying in HD mode, comparing realistic nonlinear and conventional linear EH models. Their study evaluated bit error rate, outage probability, and throughput, finding shows that both models behave similarly and provide realistic results at low harvested energy levels. The analysis did not consider the effect of interference signals on network performance. Pan & Zhu [22] investigated energy-efficient power allocation in a non-linear EH two-hop multi-relay DF cooperative system. The work evaluated the energy efficiency and harvested energy using the piecewise linear EH model under PS scheme. The results obtained showed that the piecewise linear model outperforms the conventional linear model. However, the study did not account for the impact of interfering signals on the network. The reviewed literature revealed a trade-off between tractability and accuracy in EH modelling. While the linear models are simple but lead to resource allocation mismatch, the logistic nonlinear models are analytically complex and intractable. Furthermore, prior adaptations of piecewise linear models neglect the impact of interference. This paper bridges these gaps by proposing an enhanced piecewise linear EH model that maintains tractability while incorporating interference for greater practical accuracy.

Therefore, the contributions of this work are presented as follows:

i. Proposed an enhanced piecewise linear EH model for HD AF cooperative D2D TS systems, bridging the tractability-accuracy trade-off by avoiding the overestimation of linear models and the intractability of logistic nonlinear models.
ii. Unlike prior adaptations, the proposed model explicitly accounts for the impact of interference on the formulated throughput optimization problem for AF relay assisted D2D communication

network, leading to greater practical relevance and accuracy in resource allocation.

iii. The optimization problem was solved using the Lagrange dual decomposition method and a matching resource allocation algorithm was developed.

The remainder of the paper are presented as follows. In Section 2, the method used in the proposed model was presented while Section 3 gives the result and discussion. Section 4 concludes.

2. Methodology

A. System Model

This paper investigates an amplify-and-forward (AF) relaying network, where the relay node employs a piecewise linear time-switching (TS) scheme. In the system model, a D2D transmitter, S, communicates with a D2D receiver, D, via a relay node, R. The transmission is subject to interference from a cellular user equipment (CUE), as illustrated in Fig. 1. Due to severe fading, the direct link between S and D is considered unavailable and is thus omitted from the analysis.

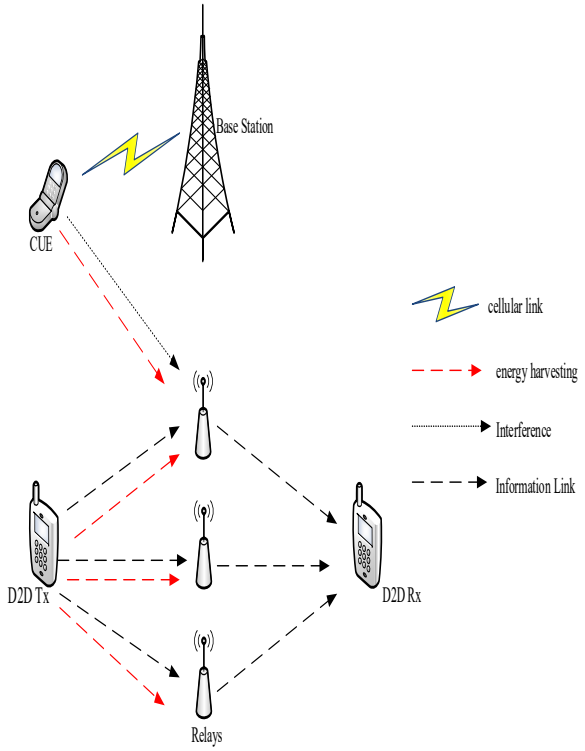

Fig.1: System model

The path loss is modeled as $d^{-\nu}$, where d denotes the distance between corresponding nodes and ν is the path loss exponent. Each wireless link experiences frequency non-selective Rayleigh block fading. It is assumed that the relay has access to instantaneous channel state information (CSI), enabled by advanced channel estimation techniques [19,23]. All nodes are equipped with a single antenna and operate in half-duplex mode. The relay is energy-constrained and harvests energy from both the D2D transmitter's signal and the interfering signal from the CUE to power its transmission. The energy consumed by relay circuitry is considered negligible compared to the energy required for D2D transmission and is therefore ignored in the analysis [24, 25].

B. Piecewise Linear Time Switching Scheme

This work studies a piecewise linear time-switching (TS) scheme to enhance the achievable throughput of a D2D network employing AF (amplify-and-forward) relaying. The protocol divides each transmission block of duration T into two phases. In the initial phase of duration αT, the D2D transmitter sends a signal, enabling the selected relay R_i to harvest energy. The remaining block time $(1-\alpha)T$ is dedicated to information transmission. This second phase is further split equally: the first half, $(1-\alpha)T/2$, is used for the source-to-relay link, and the second half for the relay-to-destination link. This frame structure is illustrated in Fig.2.

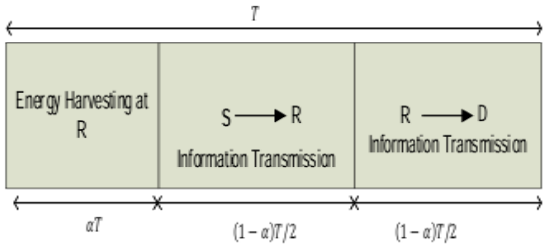

Fig.2: Time switching frame for energy harvesting and Information processing at the relay.

During the energy harvesting phase, the received signal at the ith selected relay, is given as:

$$y_{r_i}' = \sqrt{P_t^S}\, h_{Sr_i} x_s + \sqrt{P_t^C}\, h_{Cr_i} + n_{r_i} \quad (1)$$

where P_t^S and P_t^C are the respective transmit power of the D2D transmitter and CUE, respectively, h_{Sr_i} and h_{Cr_i} are the channel responses of the D2D transmitter to the ith relay and the interference link from the CUE to the D2D link, respectively. x_s is the normalised signal from D2D transmitter such that $\mathbb{E}\{|x_s(t)|^2\} = 1$ and $n_{r_i} \sim CN(0, \sigma_r^2)$ is the AWGN caused by the receiving antenna at the relay. The channel responses are obtained as:

$$h_{Sr_i} = g_{Sr_i} d_{Sr_i}^{-v} \quad (2)$$

$$h_{Cr_i} = g_{Cr_i} d_{Cr_i}^{-v} \quad (3)$$

where g_{Sr_i} and g_{Cr_i} are the Rayleigh fading channel coefficients accordingly, v is the path loss exponent corresponding to large scale fading of the transmission channel, d_{Sr_i} is the distance between the D2D transmitter and the relay node, d_{Cr_i} is the distance between the CUE and the relay node. The amount of energy harvested at the ith relay during αT using piecewise linear EH model is obtained as:

$$E_{h_i}^{TS} = \begin{cases} 0, & P_{RF}^{TS} < P_{th}^1 \\ (a_k P_{RF}^{TS} + b_k)\alpha_i T, & P_{RF}^{TS} \in \left[P_{th}^k,\ P_{th}^{k+1}\right], \\ & k = 1, \dots, N-1. \\ P_m \alpha_i T & P_{RF}^{TS} > P_{th}^N \end{cases} \quad (4)$$

The practical transmit power of the ith relay is obtained as:

$$P_{r_i} = \begin{cases} 0, & P_{RF}^{TS} < P_{th}^1 \\ \frac{2(a_k P_{RF}^{TS} + b_k)\alpha_i}{1-\alpha_i}, & P_{RF}^{TS} \in \left[P_{th}^k, P_{th}^{k+1}\right], \\ & k = 1, \dots, N-1. \\ \frac{2P_m \alpha_i}{1-\alpha_i} & P_{RF}^{TS} > P_{th}^N \end{cases} \quad (5)$$

where $P_{th} = \left\{P_{th}^k | 1 \le k \le N\right\}$ are thresholds on P_{RF}, for *N+1* linear segments, a_k and b_k are slope and intercept for linear function in the k^{th} segment, respectively. P_m denote the maximum harvestable power when the EH circuit is saturated. The input power to the energy harvester denoted by P_{RF}^{TS} given as:

$$P_{RF}^{TS} = \sqrt{P_t^S}\, h_{Sr_i} + \sqrt{P_t^C}\, h_{Cr_i} + n_{r_i} \quad (6)$$

In the second phase, the D2D transmitter transmits its signal to the relays. The signal received at the i^{th} *r*elay, which includes interference from the CUE and baseband conversion noise, is given by

$$x_{r_i} = \sqrt{P_t^S}\, h_{Sr_i} x_s + \sqrt{P_t^C}\, h_{Cr_i} + n_{r_i} + n_c \quad (7)$$

Here, $n_c \sim \mathcal{CN}(0, \sigma_c^2)$ represents the complex additive white Gaussian noise introduced during the RF-to-baseband conversion at the i^{th} relay within the CUE band. In the subsequent information transmission phase, which occupies half of the remaining time slot $(1-\alpha_i)T/2$, the relay amplifies the received signal. This amplified signal is then forwarded to the destination using the energy harvested by the relay node. Consequently, the signal received at the D2D receiver can be expressed as:

$$y_d = h_{r_i D} \beta x_{r_i} + n_d \quad (8)$$

Where $h_{r_i D} = g_{r_i D}\, d_{r_i D}^{-v}$ is the channel response between the selected relay node and D2D receiver and $g_{r_i D}$ is the complex channel coefficient, $d_{r_i D}$ is the distance between the relay node and the D2D receiver. The amplifier gain of the AF relay denoted by β is obtained as:

$$\beta = \sqrt{\frac{P_{r_i}}{P_t^S \left|h_{Sr_i}\right|^2 + P_t^C \left|h_{Cr_i}\right|^2 + \sigma_c^2 + \sigma_r^2}} \quad (9)$$

Substituting equations (7) and (9) into equation (8) gives:

$$y_d = \sqrt{\frac{P_{r_i}}{P_t^S \left|h_{Sr_i}\right|^2 + P_t^C \left|h_{Cr_i}\right|^2 + \sigma_c^2 + \sigma_r^2}}\, h_{r_i D} \left(\sqrt{P_t^S}\, h_{Sr_i} x_s + \sqrt{P_t^C}\, h_{Cr_i}\right) + \sqrt{\frac{P_{r_i}}{P_t^S \left|h_{Sr_i}\right|^2 + P_t^C \left|h_{Cr_i}\right|^2 + \sigma_c^2 + \sigma_r^2}}\, h_{r_i D} \times \left(n_{r_i} + n_c\right) + n_d \quad (10)$$

The instantaneous signal-to-interference-noise ratio (SINR) at the D2D receiver from equation (10) is obtained as:

$$\gamma_{e2e} = \frac{P_{r_i} P_t^S \left|h_{r_i D}\right|^2 \left|h_{Sr_i}\right|^2}{P_{r_i} \left|h_{r_i D}\right|^2 \left(\sigma_c^2 + \sigma_r^2 + P_t^C \left|h_{Cr_i}\right|^2\right) + \sigma_d^2 \left(P_t^S \left|h_{Sr_i}\right|^2 + P_t^C \left|h_{Cr_i}\right|^2 + \sigma_c^2 + \sigma_r^2\right)} \quad (11)$$

The achievable throughput of the cooperative network in TS scheme is given as:

$$\tau = \frac{(1-\alpha_i)T}{2} log_2(1 + \gamma_{e2e}) \quad (12)$$

C. Relay selection for TS scheme in AF relaying protocol

For the AF relaying protocol using the TS scheme, the optimal relay was selected according to an end-to-end SINR criterion at the destination. This selection, leverage on full CSI to reduce the outage performance as in [17], yields the relay index i for the TS scheme as:

$$i = \arg \max_{j_1 = 1,2,\dots M} \gamma_{e2e} \quad (13)$$

D. Problem formulation for throughput for TS scheme in AF protocol

Based on the non-linearity of practical energy harvester, an optimal dynamic TS scheme is designed to maximize the achievable throughput τ, which is obtained as:

$$\mathbf{P1}: \begin{aligned} &\max_{\alpha, P_t^S \geq 0} \quad \tau \\ &\text{s.t. C1: } 0 \leq \alpha_i \leq 1 \\ &\quad \text{C2: } 0 < P_t^S \leq P_{t(max)}^S \\ &\quad \text{C3: } 0 < P_t^c \leq P_{t(max)}^C \\ &\quad \text{C4: } P_{RF}^{TS} \geq P_{th}^1 \\ &\quad \text{C5: } P_{th}^k \leq P_{RF}^{TS} \leq P_{th}^{k+1} \end{aligned} \quad (14)$$

where C1 sets the range of the TS ratio, C2 denotes the maximum transmission power of the D2D transmitter, C3 denotes the maximum transmission power of the interference from the CUE, C4 denotes the minimum received power required for the selected relay to activate its EH circuit, which implies the EH circuit sensitivity, C5 implies that the energy harvester of the i^{th}relay, works in the k^{th} linear segment in the piecewise linear EH model.

According to the harvested energy in equation (5), three cases for the optimization problem is considered as follow:

Case 1: If $P_{RF}^{TS} < P_{th}^1$, then P_r = 0. Thus, in this case for any value of α_i, $\tau_k = 0$.

Case II: If $P_{RF}^{TS} \in [P_{th}^k, P_{th}^{k+1}]$, $\forall\, k \in \{1,\ldots, N-1\}$, the energy harvester operates in the k-*th* linear regions where $P_{r_i} = \frac{2(a_k P_{RF}^{TS} + b_k)\alpha_i}{1-\alpha_i}$ .Then τ_k is obtained as:

$$\tau_k = \frac{(1-\alpha_i)T}{2} log_2\left(1 + \frac{V_k \alpha_i}{W_k \alpha_i + Z(1-\alpha_i)}\right) \quad (15)$$

where $V_k = 2P_t^S(a_k P_{RF}^{TS} + b_k)\left|h_{r_i D}\right|^2 \left|h_{S r_i}\right|^2$

$$W_k = 2\left|h_{r_i D}\right|^2 \left(\sigma_c^2 + \sigma_r^2 + P_t^C \left|h_{C r_i}\right|^2\right)(a_k P_{RF}^{TS} + b_k)$$

$$Z = \sigma_d^2 (P_t^S \left|h_{S r_i}\right|^2 + P_t^C \left|h_{C r_i}\right|^2 + \sigma_c^2 + \sigma_r^2)$$

Case III: If $P_{RF}^{TS} > P_{th}^N$, $P_r = \frac{2P_m \alpha_i}{1-\alpha_i}$, then τ_N is obtained as:

$$\tau_N = \frac{(1-\alpha_i)T}{2} log_2\left(1 + \frac{V_N \alpha_i}{W_N \alpha_i + Z(1-\alpha_i)}\right) \quad (16)$$

where $V_N = 2P_t^S \left|h_{r_i D}\right|^2 \left|h_{S r_i}\right|^2 P_m$

$$W_N = 2\left|h_{r_i D}\right|^2 \left(\sigma_c^2 + \sigma_r^2 + P_t^C \left|h_{C r_i}\right|^2\right) P_m$$

E. Solution to the Formulated Problem

Consider the three cases from the problem formulation, the solution is obtained as follows:

Case 1: Since τ = 0, substituting for τ into problem **P1,** the solution to problem **P1** gives zero for any value of α_i and P_t^S.

Case II: Based on equations (15) and (16) when $P_{RF}^{TS} \geq P_{th}^1$, then τ_k in the k-th, $\forall\, k \in \{1,\ldots, N\}$ linear region is same as in equation (15) assume that $T = 1s$, then the problem can be written as:

$$\mathbf{P2}: \max_{\alpha_i, P_t^S} \frac{(1-\alpha_i)}{2} log_2\left(1 + \frac{V_k \alpha_i}{W_k \alpha_i + Z(1-\alpha_i)}\right) \quad (17)$$
$$s.t.\ C1 - C5$$

Employing Lagrange dual decomposition to solve **P2,** the Lagrange function is given by:

$$L(P_t^S, \alpha_i, \beta_1, \delta_1, \emptyset_1, \epsilon_1) = \tau_k - \beta_1(\alpha_i - 1) - \delta_1\left(P_t^S - P_{t(max)}^S\right) - \emptyset_1(P_t^c - P_{t(max)}^C) + \epsilon_1\left(P_{RF}^{TS} - P_{th}^1\right) \quad (18)$$

where $\beta_1, \delta_1, \emptyset_1$ and ϵ_1 are Lagrange multipliers for C1-C4, respectively. Then the dual optimization problem is obtained as:

$$\mathbf{P3}: \min_{(\beta_1, \delta_1, \emptyset_1, \epsilon_1 \geq 0)} \max_{(\alpha_i, P_t^S)} L(P_t^S, \alpha_i, \beta_1, \delta_1, \emptyset_1, \epsilon_1)$$
$$\text{s.t. C5.} \quad (19)$$

The following proposition is a part devoted to solving **P3.**

Proposition 1: Based on equation (19), **P3** is convex with regard to α_i when P_t^S is fixed. Similarly, **P3** is a convex problem with respect to P_t^S when α_i is fixed.

Proof: See Appendix A.

Based on proposition 1, the local optimal α_i^*, can be determined for a given P_t^S, using Karush-Kuhn-Tucker (KKT) conditions to obtain the expression for α_i^*, where *T*=1s as $\frac{\partial L(P_t^S, \alpha_i, \beta_1, \delta_1, \emptyset_1, \epsilon_1)}{\partial \alpha_i}$ = 0.

Obtaining $L(P_t^D, \alpha_i, \beta_1, \delta_1, \emptyset_1, \epsilon_1)$ with regards to α_i, using KKT condition gives:

$$\frac{1}{2} log_2\left(1 + \frac{V_k \alpha_i}{W_k \alpha_i + Z(1-\alpha_i)}\right) + \beta_1 = \frac{V_k Z(1-\alpha_i) log_2^e}{2(W_k \alpha_i + Z(1-\alpha_i) + V_k \alpha_i)(W_k \alpha_i + Z(1-\alpha_i))} \quad (20)$$

Observation from equation (20), shows that α_i can only be solved numerically. Similarly, to obtain the locally optimal P_t^S for the optimized α_i, then the first order derivative of $L(P_t^S, \alpha_i, \beta_1, \delta_1, \emptyset_1, \epsilon_1)$ with regards to P_t^S is obtained. Equation (18) can be re-written as:

$$L(P_t^S, \alpha_i, \beta_1, \delta_1, \emptyset_1, \epsilon_1) =$$

$$A log_2\left(1 + \frac{V' P_t^S}{W' + B P_t^S + Z'}\right) - \beta_1(\alpha_i - 1) - \delta_1\left(P_t^S - P_{t(max)}^S\right) - \emptyset_1(P_t^c - P_{t(max)}^C) + \epsilon_1\left(P_{RF}^{TS} - P_{th}^1\right) \quad (21)$$

where $A = \frac{(1-\alpha_i)}{2}$, $V' = 2\alpha_i(a_k P_{RF}^{TS} + b_k)\left|h_{r_i D}\right|^2 \left|h_{S r_i}\right|^2$,
$W' = 2\left|h_{r_i D}\right|^2 \left(\sigma_c^2 + \sigma_r^2 + P_t^C \left|h_{C r_i}\right|^2\right)(a_k P_{RF}^{TS} + b_k)\,\alpha_i$,
$B = \sigma_d^2(1-\alpha_i)\left|h_{D r_i}\right|^2$,
$Z' = \sigma_d^2(P_t^C \left|h_{C r_i}\right|^2 + \sigma_c^2 + \sigma_r^2)\,(1-\alpha_i)$.
With $W'' = W' + Z'$, therefore equation (21) becomes:

$$L\left(P_t^S,\alpha_i,\beta_1,\delta_1,\emptyset_1,\epsilon_1\right)=\ Alog_2\left(1+\frac{V'P_t^S}{W''+BP_t^S}\right)-\beta_1(\alpha-1)-\ \delta_1\left(P_t^S-P_{t(max)}^S\right)-\emptyset_1(P_t^c-P_{t(max)}^C)+\epsilon_1\left(P_{RF}^{TS}-P_{th}^1\right) \quad (22)$$

Therefore, obtaining $L\left(P_t^S,\alpha_i,\beta_1,\delta_1,\emptyset_1,\epsilon_1\right)$ with regards to P_t^S, when α_i is fixed, gives the optimal values of P_t^S, this can be obtained by solving the equation (22) by applying the KKT condition $\frac{\partial L(P_t^S,\alpha_i,\beta_1,\delta_1,\emptyset_1,\epsilon_1)}{\partial P_t^S}=0$.

Equation (22) can be obtained in quadratic form as:

$$c_1{P_t^S}^2+\ c_2P_t^S+c_3=0 \quad (23)$$

Therefore, the optimal value of P_t^S, in **P3** is obtained as:

$$P_t^{S^*}=\frac{-c_2\pm\sqrt{c_2^2-4c_1c_3}}{2c_1} \quad (24)$$

where $c_1=\ (-\delta_1+\epsilon_1\left|h_{Sr_i}\right|^2)B(B+\ V')$

$$c_2=\ (-\delta_1+\epsilon_1\left|h_{Sr_i}\right|^2)W''(2B+V')$$

$$c_3=\ AV'W''log_2^e+\ (-\delta_1+\ \epsilon_1\left|h_{Sr_i}\right|^2)W''^2$$

Therefore, the solution to equation (24) is based on two cases as:

Case 1: If $c_2^2-4c_1c_3=0$, there exist two equal real roots.

Case 2: If $c_2^2-4c_1c_3>0$ there exist two real roots.

Then gradient method is used to update the values of the Lagrange multipliers as follows:

$$\begin{aligned}\beta_1(t+1)&=\{\beta_1(t)+s_1(\alpha_i-1)\}^+\\ \delta_1(t+1)&=\left\{\delta_1(t)+s_2\left(P_t^S-P_{t(max)}^S\right)\right\}^+\\ \emptyset_1(t+1)&=\left\{\emptyset_1(t)+s_3(P_t^c-P_{t(max)}^C)\right\}^+\\ \epsilon_1(t+1)&=\left\{\epsilon_1(t)-s_4\left(P_{RF}^{TS}-P_{th}^1\right)\right\}^+\end{aligned} \quad (25)$$

Where s_1, s_2, s_3 and s_4 are the step sizes for the linked constraints and are needed to be adequately initialized in order to guarantee convergence and optimality. Also, t is the iteration index. In this paper, the step size for updating the Lagrange multipliers is set as 10^{-5}. An iterative algorithm given in Algorithm 1 is used to determine the optimal α_i and P_t^S. The segment that maximizes the throughput of the TS enabled relay aided D2D link is obtained by $k^*=\arg max\{\tau_1,\tau_2\dots\dots\dots,\tau_N\}$. The algorithm also performs the relay selection scheme based on full CSI of the link, where the maximum number of iterations is denoted by l. The iteration terminates when the difference between the value of the achieved throughput and that of the previous throughput in previous step is smaller than φ. The maximum number of linear segments is denoted by N_{max}.

Algorithm 1: Determination of Optimal value of $P_t^{S^*}$ and $\alpha_i{}^*$ that maximizes the Throughput

1: **Begin**
2: **Set parameters**: $\left\{P_{th}^k\right\}_{k=1}^N, P_t^S, P_{t(max)}^C, \sigma_r^2, \sigma_c^2, \sigma_d^2, \{a_k\}_{k=1}^{N-1}, \{b_k\}_{k=1}^{N-1}, \ i=1,2,3\dots M, \varphi, t=0;$
3: **Input**: CSI, h_{Cr_i}, h_{Sr_i} and h_{r_iD}:
4.Output: $P_t^{S^*},\ \alpha_i{}^*, \tau_k$
5: Initialize: the maximum number of iterations
6: Compute P_{RF}^{TS};
7: **if** $P_{RF}^{TS}<P_{th}^1$, then P_r = 0, $\tau=0$ and flag = 0;
8: **else**
9: flag =1
10: **While** $P_{th}^k\le P_{RF}^{TS}\le P_{th}^N$;
11: set $t=t+1$
12: **for** $k=1$: N_{max} **do**
13: initialize value of P_t^S to obtain $\alpha_i{}^*$ by calculating equation (21)
14: **while** $t\ <l$ **do**
15: use the achieved value of $\alpha_i(t)$ to obtain $P_t^S(t+1)$ based on proposition 1 and use equation (24)
16: use the calculated $P_t^S(t+1)$ to obtain $\alpha_i(t+1)$ based on proposition 1 and use equation (21)
17: **if** $\tau_k(t+1)-\ \tau_k(t)\ <\ \varphi$ **then**
18: $\tau_k(t+1)=\frac{(1-\alpha_i)}{2}log_2(1+\ \gamma_{e2e}(t+1)\ )$
19: update Lagrange multipliers using (25)
20: **continue**
21: **else**
22: $P_t^S=P_t^S(t+1), \alpha_i=\ \alpha_i(t+1), \tau_k=\tau_k(t+1)$
23: **end if**
24: **end while**
25: **end for**
26: **end while**
27: **end if**
28: **while** $P_{RF}^{TS}\ \ge\ P_{th}^1$
29: obtain $P_{RF\,TS}^{max}$ and decide the maximum number of segments: N_{max}
30: **for** k=1: N_{max} **do**
31: $j^*=\arg max\{\tau_1,\tau_2\dots\dots\dots,\tau_N\}$
32: obtain $P_t^{S^*}, \alpha_i^*$and τ_k
33: **end for**
34: **for** i=1: M , $k=1$: N_{max} **do**
35: compute the index of the selected relay based on equation (13)
36: **end for**
37: **end while**
38: End

3. Results and Discussion

This section presents simulation results to demonstrate how optimal throughput is achieved in the proposed piecewise linear model for an AF relaying network. The analysis leverages the derived closed-form expressions,

showing how throughput depends on the TS ratio and the D2D transmitter's power. Simulation parameters are listed in Table 1. To obtain the maximum throughput, the mathematical model formulated in Equations (18) and (22) was solved using Lagrangian duality and KKT conditions. The model was then simulated and averaged over 100 runs in MATLAB R2021a. The corresponding results are shown in Figures 3 to 5.

Fig. 3 illustrates the relationship between Input RF Power and harvested DC power for different EH models. The Linear model significantly overestimates harvested power, as it fails to capture the nonlinear saturation effects of practical rectification, despite its analytical simplicity.

Table 1. Simulation parameters

Parameter	Value
Path loss exponent, ν	3
Maximum transmission power, of source $P^{S}_{t(max)}$	30dBm
Transmission Power, of CUE $P^{C}_{t(max)}$	30dBm
Noise power σ_r^2, σ_P^2, σ_d^2, σ_c^2	-100dBm
Receiver power segment $[P^0_{th}, P^1_{th}, P^2_{th}, P^3_{th}]$, with $N = 3$	[0,20, 35, 50] mW
Coefficient $[a_o, a_1, a_2, a_3]$,	[0.34, 0.553, 0.584, 0]
Intercept $[b_o, b_1, b_2, b_3]$	[0,-4.266, -5.34, 23.8]mW
Receiver power segment $[P^0_{th}, P^1_{th}, P^2_{th}, P^3_{th}, P^4_{th}]$, with $N = 4$	[0, 20, 35, 40, 50] mW
Coefficient $[a_o, a_1, a_2, a_3, a_3]$	[0, 0.68, 0.454, 0.463,0]
Intercept $[b_o, b_1, b_2, b_3]$	[0.3,-6.8,1.11, 7, 24]mW
Circuit Power consumption, P_C	20dBm

In contrast, the proposed piecewise linear model with k=4 demonstrates high accuracy, closely aligning with the measured data [26], followed by the k=3 variant. As shown, increasing the number of segments improves the approximation of the smooth nonlinear curve, making the piecewise linear approach both accurate and mathematically tractable for optimization. This superior fit explains why the resource allocation algorithm based on the k=4 model achieved higher throughput in your earlier results. By accurately representing real-world energy harvesting behavior, the algorithm can make better decisions—such as selecting the optimal TS ratio of 0.29, leading to improved performance.

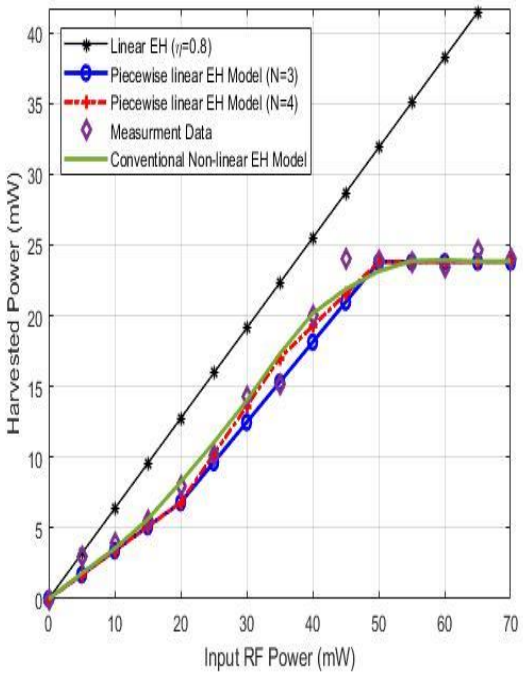

Fig.3: Harvested power against Input RF power

Fig. 4 shows how average throughput varies with the TS ratio under different EH models. The proposed piecewise linear model performs best, with its k=4 variant outperforming the conventional nonlinear and linear models. At a TS ratio of 0.22, the k=4 model achieves 1.53 bps/Hz, compared to 1.41 bps/Hz for k=3, 1.10 bps/Hz for conventional nonlinear and 0.98 bps/Hz for the linear model. While the conventional models peaked at TS ratio of 0.22, the proposed piecewise linear models reach maximum throughput at TS ratio of 0.29. This confirms that the resource allocation optimized for the proposed piecewise linear EH model is more effective. Moreover, increasing the number of segments in the model steadily improves allocation performance.

Fig. 5 compares average throughput versus D2D transmitter power for different EH models. The proposed piecewise linear model consistently outperforms the others, particularly at a TS ratio of 0.2. Its peak throughput occurs at a TS ratio of 0.29. For instance, at the transmit power of 18.24 dBm, the average throughputs obtained were 0.88, 0.84, 0.64, and 0.55 bps/Hz for k=4, k=3, nonlinear, and linear models, respectively. The throughput rises with power for all models, converging near 28.24 dBm for the optimal transmit power. At this point, the throughputs reach 1.54, 1.48, 1.13, and 0.98 bps/Hz for k=4, k=3,

nonlinear, and linear models, respectively. The proposed piecewise linear model, especially the k=4 variant, maintains a clear advantage due to its refined segmentation and supporting resource allocation algorithm.

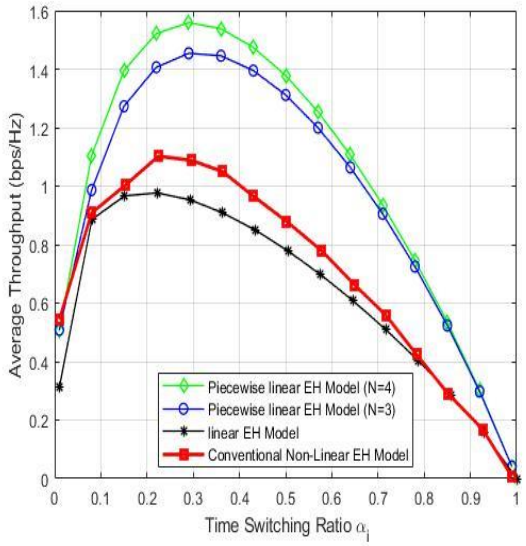

Fig.4: Average Throughput versus TS ratio

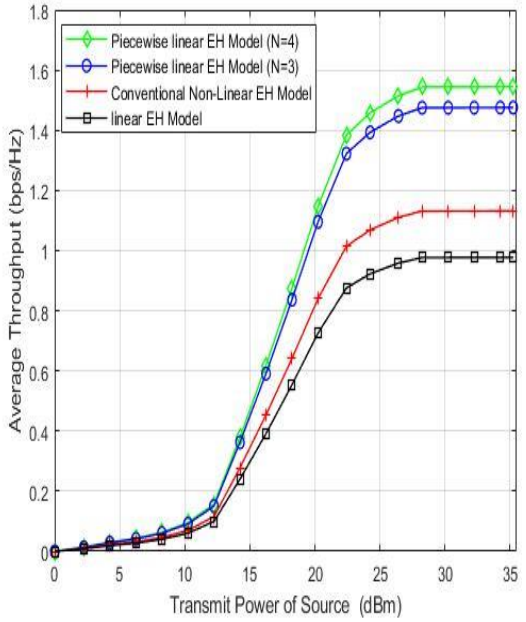

Fig.5: Average throughput versus transmit power of D2D sources

4. Conclusion

This paper has presented the piecewise linear TS scheme for an AF relaying protocol in cooperative D2D network. A throughput optimization problem was formulated and constrained to instantaneous network resources. The formulated problem was solved using the Lagrange dual decomposition method. Simulation results demonstrated that the proposed piecewise TS scheme outperforms the conventional linear and non-linear EH models in terms of throughput performance.

Author contributions

Gbenga Ayodeji Gbotoso: Writing-Original draft preparation, Methodology, Software and Writing-Reviewing

Damilare Oluwole Akande: Data Curation, Editing and Investigation.

Zachaeus Kayode Adeyemo: Conceptualization and Validation

Conflicts of interest

The authors declare no conflicts of interest.

APPENDIX A

Proof of Proposition 1

In order to obtain the convexity of the optimization problem in equation (20). The second-order derivative of the Lagrange function $L\ (P_t^S, \alpha_i, \beta_1, \delta_1, \emptyset_1, \epsilon_1)$ with regard to α_i, with P_t^S regarded as a fixed value, where T=1s, is derived. The Lagrange function is denoted as L for simplicity. The second-order derivative is obtained as:

$$\frac{\partial^2 L}{\partial {\alpha_i}^2} = \frac{-\left({V_k}^2+2V_kW_k\right)Z^2(1-\alpha_i)-2W_k\left({V_k}^2+V_kW_k\right)Z\alpha_i}{2(Z(1-\alpha_i)+W_k\alpha)^2(Z(1-\alpha_i)+(V_k+W_k)\alpha_i)^2\ln 2} \quad (A.1)$$

Based on equation (A.1), all variables and constants are greater than zero, therefore $\frac{\partial^2 L}{\partial {\alpha_i}^2}$ <0 will always hold for 0 < α <1, which makes **P3** to be convex. Similarly, when $\alpha_i$is fixed, the second-order derivative of L with regard to P_t^S is obtained as:

$$\frac{\partial^2 L}{\partial {P_t^S}^2} = -\frac{2ABV'W''^2+2AB^2P_t^SV'W''+AV'^2W''^2+2ABP_t^SV'^2W''}{\left(W'^2+2BP_t^SW''+B^2P_t^{S^2}+P_t^S\,V'W''+BP_t^{S^2}V'\right)^2\ln 2} \quad (A.2)$$

All variables and constants in equation (A.2) are greater than zero, $\frac{\partial^2 L}{\partial {P_t^S}^2} < 0$, so the optimization problem is convex with regard to P_t^S when α_i is fixed. Therefore, combining equations (A.1) and (A.2), proposition 1 is proven.

References

[1] Yang, H., Ye, Y., Chu, X., & Dong, M. (2020). Resource and Power Allocation in SWIPT-Enabled

Device-to-Device Communications Based on a Nonlinear Energy Harvesting Model*. IEEE Internet of Things Journal*, 7(11), 10813–10825. https://doi.org/10.1109/JIOT.2020.2988512

[2] Liu, X., & Ansari, N. (2017). Green Relay Assisted D2D Communications with Dual Batteries in Heterogeneous Cellular Networks for IoT. *IEEE Internet of Things Journal*, 4(5),1707–15.

[3] Li, Y., Chi K, Chen, H., Wang, Z., & Zhu, Y. (2018). Narrowband Internet of things Systems with Opportunistic D2D Communication. *IEEE Internet of Things Journa*l,5(3),1474–84.

[4] Chettri, L., & Bera, R. (2020). A comprehensive Survey on Internet of Things (IoT) toward 5G Wireless Systems*. IEEE Internet of Things Journal*, 7(1), 16-32,

[5] Kuang, Z., Liu, G., Li, G., & Deng, X. (2019). Energy Efficient Resource Allocation Algorithm in Energy Harvesting-based D2D Heterogeneous Networks. *IEEE Internet of Things Journal*, 6(1), 557-567.

[6] Akande, D. O., Ojo, F. K., Ojo, S. I. & Oseni, O. F. (2025). Adaptive Cooperative MAC with Energy Harvesting for Multi-Objective Performance in Wireless Ad-hoc Networks, *Nigerian Journal of Technological Developmen*t, 22(4): 113-124.

[7] Tang, J., So, D.K.C., Zhao, N. Shojaeifard, A., & Wong, K.K. (2017), Energy Efficiency Optimization with SWIPT in MIMO Broadcast Channels for Internet of Things, *IEEE Internet of Things Journal*, 5(4), 2605 - 2619.

[8] Tang, J., So, D.K.C., Shojaeifard, A. Wong, K.K., & Wen, J. (2017). Joint Antenna Selection and Spatial Switching for Energy Efficient MIMO SWIPT system. IEEE Transactions on Wireless Communication, 16(7), 4754-4769,

[9] Shi, L., Zhao, L., Liang, K., & Chen, H.H. (2018) Wireless Energy Transfer Enabled D2D in Underlaying Cellular networks*. IEEE Transactions on Vehicular Technology*, 67(2), 1845-1849.

[10] Ye, J., Lei, H., Liu, Y., Pan, G.,da Costa, D. B., Ni, Q., & Ding, Z. (2017). Cooperative communications with Wireless Energy Harvesting over Nakagami-m Fading Channels. *IEEE Transaction on Communications*, 65(12), 5149-5164.

[11] Nasir, A.A., Zhou, X., Durrani, S., & Kenedy, R.A.(2013). Relaying Protocols for Wireless Energy Harvesting and Information Processing at the Relay. *IEEE Transactions on Wireless Communications*, 12(7), 3622-3636.

[12] Ye, Y., Li, y., Wang, D., & Lu, G. (2017). Power Splitting Protocol Design for the Cooperative NOMA with SWIPT, *in Proceedings of IEEE International Conference on Communications*, pp.15.

[13] Ojo, F. K., Akande, D. O., & Salleh M. F. M. (2018). An Overview of RF Energy Harvesting and Information Transmission in Cooperative Communication Networks, *Telecommunication Systems, 70(2): 295-308.*

[14] Akande, D. O., & Salleh M. F. M. (2020). A Multi-Objective Target-Oriented Cooperative MAC Protocol for Wireless Ad-hoc Networks with Energy Harvesting, *IEEE Access*, 8: 25310-25325.

[15] Vu, V. So Dinh, T. D., Tran, M. H., Do, T. Q. and Pham, T. H. (2020). Analysing outage probability of linear and non-linear RF energy harvesting ofcooperative communication networks, *IET Signal Processing*, 14(8):541-550.

[16] Salim, M.M., Elsayed, H.A., Abdalzaher, M.S & Fouda, M.M. (2023). RF Energy Harvesting Effectiveness in Relay-based D2D Communication, " *2023 International Conference on Computer Science, Information Technology and Engineering (ICCoSITE),* Jakarta, Indonesia, 342-347.
doi: 10.1109/ICCoSITE57641.2023.10127846.

[17] Boshkovska, E., Ng, D. W. K., Zlatanov, N., and Schober, R. (2015). Practical Non-linear Energy Harvesting model and Resource Allocation for SWIPT Systems. *IEEE Communications Letters*, 19(12):2082–2085.

[18] Bai, X., Shao, J., Tian, J., & Shi, L. (2018). Power-Splitting Scheme for Nonlinear Energy Harvesting AF Relaying with Direct Link. *Wireless Communications and Mobile Computing*, 2018, 7906957.

[19] Kader, M.F., and Mahmood, M.A.I. (2025). Linear and Nonlinear Energy Harvesting in Concurrent Cellular and D2D Communication. *Wiley Engineering Reports*, 1:1-11.

[20] Lu, G., Shi, L., & Ye, Y.(2018). Maximum Throughput of TS/PS Scheme in an AF Relaying Network with Non-Linear Energy Harvester. *IEEE Access*, 6, 26617–26625

[21] Babaei, M., Durak-Ata, L., & Aygölü, Ü. (2022). Performance Analysis of Dual-Hop AF Relaying with Non Linear/Linear Energy Harvesting. *Sensors*, 22(5987), 1-24

[22] Pan, H. & Zhu, Q. (2021). Energy-Efficient Power Allocation in Non-Linear Energy Harvesting

Multiple Relay Systems. *Algorithms* 2021, 14, 155

[23] Cvetkovic, A., Blagojevic, V., & Ivani, P. (2017). Performance Analysis Of non-linear Energy-Harvesting DF Relay System in interference-Limited Nakagami-m Fading Environment. *ETRI Journal*, 39(6), 803-812.

[24] Zhang, J.L., & Pan, G.F. (2016). Outage analysis of wireless-powered relaying MIMO systems with non-linear energy harvesters and imperfect CSI, *IEEE Access*, 4: 7046-7053.

[25] Wang, K., Li, ., Ye, Y., Li, Y., & Zhang, H. (2017). Dynamic Power Splitting Schemes for non-linear EH Relaying Networks: Perfect and Imperfect CSI. *Proceedings of IEEE Vehicular Technology Conference*, 15.

[26] Guo, J., & Zhu, X. (2012) An Improved Analytical Model For RF-DC Conversion Efficiency in microwave Rectifiers. *In Proceedings of the 2012 IEEE/MTT-S International Microwave Symposium* , 1:1–3.